JOURNAL OF CATALYSIS 138, 694–713 (1992)

Methanol Synthesis over Catalysts Derived from $CeCu_2$: Transient Studies with Isotopically Labelled Reactants

A. P. WALKER,*,[1] R. M. LAMBERT,*,[2] R. M. NIX,† AND J. R. JENNINGS‡

*Department of Chemistry, University of Cambridge, Lensfield Road, Cambridge CB2 1EW, United Kingdom; †Department of Chemistry, Queen Mary and Westfield College, University of London, London E1 4NS, United Kingdom; and ‡I.C.I. plc, Chemicals & Polymers Group, Research Department, P.O. Box 90, Wilton, Middlesbrough, Cleveland TS6 8JE, United Kingdom

Received April 3, 1992; revised June 23, 1992

The transient response of activated $CeCu_2$-derived methanol synthesis catalysts to pulses of isotopically labelled CO, CO_2, and O_2 has been determined under a variety of conditions. These data are supplemented by appropriate H/D exchange and TPD measurements. The results confirm previous studies on related catalysts showing that methanol is synthesized by hydrogenation of CO and not CO_2. They also show that the active catalyst surface is extensively covered with a hydrogen-deficient methanol precursor under steady-state conditions and that the cerium oxide surface or its interface with the copper crystallites is intimately involved in the synthesis process. Transient exposure to oxidizing gases (e.g., CO_2 and O_2) causes displacement of the precursor, giving an increased yield of methanol. Higher levels of exposure lead to the formation of strongly bound CO_2-derived complexes on the oxide surface: these quench the high synthesis activity.

INTRODUCTION

Catalysts derived from intermetallic compounds of the rare earths (RE) are highly active for a wide range of important reactions (*1–4*). Copper-containing alloys, in particular, show great promise as precursors for low-temperature methanol synthesis catalysts (*5–7*). *In situ* XRD studies of the activation of Ce–Cu and Nd–Cu intermetallics revealed that the CO/H_2 reactant gas feed induces extensive transformation of the starting material to yield an active catalyst containing crystallites of rare earth oxide and metallic copper (*7*). Thus activation of the alloy may be carried out in the reactor and is immediately followed by the onset of methanol synthesis. This work indicated that XRD-invisible, highly dispersed copper entities in intimate contact with the rare earth oxide support phase are responsible for the extraordinarily high activity of these catalysts. A recent *in situ* EXAFS study (*8*) of the activation and performance of $CeCu_2$-alloy-derived catalysts showed that the copper was largely present as ~20–25 Å particles, which would indeed be undetectable by XRD.

Industrial implementation of such alloy-derived catalysts is impeded by their adverse response to the presence of carbon dioxide in the gas feed: even very low levels (<2%) of CO_2 induce a significant decrease in the activity of methanol synthesis catalysts derived from Nd–Cu and Ce–Cu alloys (*9*). Indeed, the $CeCu_2$-derived system appears to undergo complete and irreversible poisoning when exposed to a CO_2-containing feed, while the methanol activity of the $NdCu_2$-derived catalyst falls to zero in the presence of CO_2, but recovers slightly when the CO_2 is removed (*7, 9*).

This behaviour stands in marked contrast with that of the conventional $Cu/ZnO/Al_2O_3$ industrial catalyst for which the presence of CO_2 is essential to obtain and maintain high

[1] Present address: Johnson Matthey Technology Centre, Blount's Court, Sonning Common, Reading RG4 9NH, United Kingdom.

[2] To whom correspondence should be addressed.

0021-9517/92 $5.00

activities. Indeed, in some cases the CO_2 level in the syn-gas feed exceeds that of CO (*10*). Furthermore, it has been demonstrated that conventional catalysts generate methanol almost exclusively *from* CO_2 under industrial conditions (*11, 12*); Cu/RE-derived catalysts generate methanol *from CO* (*9*).

More recent work on RE-containing, alloy-derived Cu catalysts (*13*) has shown that the effects of CO_2 exposure are strongly dependent upon the experimental conditions employed. Pulsing of CO_2 into the CO/H_2 feed gas to such catalysts was found to result in a significant, transient *increase* in the methanol concentration in the exit gas, with no apparent detrimental effect on the steady-state activity. Similar effects were observed when O_2 or N_2O were pulsed into the feed gas (*13*).

This paper describes pulsing experiments in which *isotopically labelled* gases were employed to elucidate details of the methanol synthesis reaction over $CeCu_2$-derived catalysts. The mechanisms by which CO_2 and oxygen both transiently enhance the methanol yield and ultimately poison the system have also been investigated.

EXPERIMENTAL

Experiments were carried out in a modified version of a microreactor which has been described previously (*14*). The single-pass, fixed-bed reactor consisted of a $\frac{1}{4}$" o.d. stainless steel tube contained within an aluminium-bronze heater block. A pulsing loop, of internal volume 2 cm^3, was incorporated into the microreactor just upstream of the reactor tube. Product analysis was performed using a multiplexed quadrupole mass spectrometer: the system allowed up to 11 masses to be monitored simultaneously and also recorded the temperature and flow rate through the catalyst bed. For some experiments, a sheathed thermocouple (1 mm diameter) was incorporated in the catalyst bed; more typically, the thermocouple was placed in contact with the outside of the reactor tube, within the heater block, aligned with the centre of the catalyst bed. A calibration run with one thermocouple within the catalyst bed and one in contact with the outside of the reactor tube showed no significant difference in recorded temperature over the range of relevance to the present work.

The $CeCu_2$ alloy was prepared by high-vacuum, electron-beam melting as described previously (*7*). For each experiment 0.45 g of alloy was crushed in an argon atmosphere to a particle size of 50–250 μm. This was then mixed with 2 g of 300-μm glass beads to accommodate the expansion associated with the alloy-to-catalyst transformation, and loaded into the reactor tube. A further 0.3 g of beads was loaded on top of the diluted sample in order to preheat the reactant gas stream. The tube was then sealed and transferred to the microreactor.

Reactant gases were obtained from BOC Ltd. Special Gases and used without additional purification: hydrogen (CP grade, ≥99.999% pure), premixed CO/H_2 (33/67-impurities $O_2 \leq 5$ ppm, $H_2O \leq 2$ ppm and $CO_2 \leq 20$ ppm), premixed $CO/CO_2/H_2$ (32/2/64-impurities $O_2 \leq 3$ ppm and $H_2O \leq 10$ ppm), and nitrogen (CP grade, ≥99.999% pure). Helium (CP grade, ≥99.999% pure) was further purified by passage through a molecular sieve column at room temperature. Pulsing experiments were carried out using: CO, CO_2, O_2 (Research Grade—BOC Ltd. Special Gases); D_2 (CP grade, 99.8 atom%—Cambrian Gases); ^{13}CO, $C^{18}O$, $^{13}CO_2$ (99 atom%—Cambrian Gases); and $^{18}O_2$ (99 atom%—Amersham International plc); $C^{18}O_2$ (97 atom%–Cambrian Gases). Cerium carbonate (99.9%) was obtained from Rare Earth Products Ltd.

The *in situ* activation process and subsequent steady-state activity measurements were both carried out using the (1 : 2) CO/H_2 mixture at 20 bar pressure. Steady-state activities are quoted in mol(MeOH)/kg(cat) · h and space velocities are calculated using the volume of the alloy precursor before activation. Pulsing experiments into CO/H_2 were performed by filling the loop to ~1 bar

(absolute) pressure with the desired gas and then sweeping out this volume with the 20-bar reactant gas mixture. In some cases when unlabelled CO, CO_2, and O_2 were used, a higher pulsing pressure was employed. Pulsing experiments into H_2 alone were carried out at 14 bar so that the hydrogen partial pressure over the catalyst was similar for both the CO/H_2 and H_2 work. Pulsing into He was also performed at 14 bar to facilitate a direct comparison with the corresponding H_2 data. In general, data acquisition was started 60 s before pulse injection, to establish the baseline levels of the relevant species. Runs were terminated after 15–20 min, when the effects of the pulse had died away and the system had returned to steady state. For TPD experiments the catalyst was cooled to room temperature under the reaction gas mixture. The feed was then switched to pure He carrier gas at 1 bar (flow rate ~40 sccm) and the temperature ramped linearly at 30°C/min to 480°C. After such measurements, the catalyst was discharged and a fresh charge of alloy activated. Surface area measurements were not carried out owing to difficulties encountered in ensuring satisfactory and reproducible outgassing of the catalyst samples, without induced thermal deactivation (*14*).

Mass spectral data are presented in raw form, i.e., without background subtraction or correction for interference from fragment ion signals. Traces in the figures are annotated with the corresponding atomic mass value, followed by the relative gain in parentheses. Unless specifically mentioned, no digital processing was performed. Control experiments gave the following relative intensities for the principal ions in the methanol spectrum: 29(CHO) : 30(CHOH) : 31(CH_2OH) : 32(CH_3OH) ~76 : 10 : 100 : 63.

RESULTS AND DISCUSSION

Steady-State Activation, CO Pulsing, and H/D Exchange

The initial activity of $CeCu_2$-derived methanol synthesis catalysts can be increased by hydrogen pretreatment (*14*). The precursor alloy was therefore initially exposed to 15 bar H_2 at 100°C for 2 h. The gas feed was then switched to 20 bar CO/H_2 and the temperature ramped to 180°C at 20°C/min—Fig. 1 shows the response of the system. *In situ* XRD experiments (*7*) showed that H_2 pretreatment at low temperatures transforms the initial alloy into a mixture of intermetallic hydride phases. These are highly reactive and induce rapid dissociation of CO upon exposure to the synthesis gas feed. The oxygen is principally incorporated into the solid, resulting in formation of a substoichiometric CeO_x phase. The hydrogen liberated during this intermetallic hydride-to-CeO_x conversion step, along with the gas-phase hydrogen, reacts with the CO-derived carbon on the surface: this process leads to the methane transient illustrated in Fig. 1. The incorporation of some

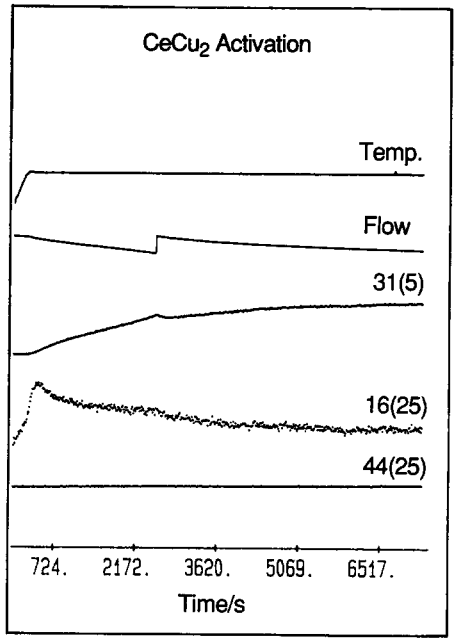

FIG. 1. *In situ* activation of $CeCu_2$ precursor alloy in 20 bar (1 : 2) CO/H_2 upon raising the temperature from 100 to 180°C, showing initial CH_4 transient associated with the activation process and subsequent increase in methanol production. Annotation of mass spectrometer signal traces is: mass number (amplifier gain factor).

carbon into the oxide phase cannot be ruled out; it is also likely that a reservoir of hydrogen is retained within the substoichiometric CeO_x support phase. An adjustment in flow rate after ~2500 s (Fig. 1) was made to compensate for the gradual drop in flow resulting from sample expansion. The steady-state activity of this CeO_x/Cu catalyst was ~16.4 moles MeOH (STP) · kg^{-1} · h^{-1} (selectivity >95%) at a standard space velocity of 28,000 h^{-1}. The principal by-product was methane (<5%), although this may have included a contribution from continued activation of residual alloy precursor.

Following the attainment of steady-state activity at 180°C, the gas feed was switched isothermally from synthesis gas to pure hydrogen. As noted above, the hydrogen pressure (14 bar) was such that no significant change in the hydrogen partial pressure was associated with the switch. Once the reactor had been purged with H_2, a pulse of CO was injected into the hydrogen stream: the resulting product distribution is shown in Fig. 2A. The only species observed were methanol and unreacted CO. No exotherm was associated with the CO pulse, so the methanol observed was not simply being desorbed thermally. It was also found that CO pulsing into a hydrogen stream at a lower flow rate resulted in the observation of a larger quantity of methanol. This is to be expected in view of the longer contact time.

The nature of the processes occurring was investigated further by activating a new catalyst sample, purging with H_2, and injecting a pulse of ^{13}CO into the hydrogen stream. Owing to a low level of $^{13}C^{18}O$ impurity in the ^{13}CO, the parent ion of methanol was used for analysis. Figure 2B shows the traces for selected signals resulting from the ^{13}CO pulse into H_2. As previously observed in Fig. 2A, some of the pulsed CO passed through the system unreacted; a small amount of displaced ^{12}CO was also detected. However, *no $^{13}CH_3OH$ (m/e = 33) was observed,* whereas a large quantity of $^{12}CH_3OH$ was detected. This clearly shows that the methanol observed when CO is pulsed into an H_2 gas stream is *not* being formed by the direct reaction of the pulsed CO with H_2–in fact, *the CO displaces methanol from the catalyst.* The pulsed ^{13}CO which sticks to the surface (displacing the preformed methanol) does not itself react rapidly with H_2 to form methanol since no $^{13}CH_3OH$ is observed. Therefore, under methanol synthesis conditions, the active surface of the catalyst would appear to be covered to a very large extent by either adsorbed methanol product or a strongly bound methanol precursor.

Further ^{13}CO pulses passed over the catalyst resulted in the eventual appearance and growth of a peak at m/e = 33 ($^{13}CH_3OH$). However, as is apparent from Fig. 2C (data from the 20th pulse) the methanol observed is still principally $^{12}CH_3OH$. Clearly the CO which remains on the catalyst after each pulse is incorporated into a very large precursor pool, so that the level of ^{13}C-containing precursors increases only gradually and there is a significant delay before $^{13}CH_3OH$ can be detected.

Additional information about the nature of the precursor was obtained from a catalyst activated in the usual way and then purged, at reaction temperature, with 14 bar He. Figure 2D illustrates the effect of pulsing ^{13}CO into this helium stream: *no methanol, either ^{12}C- or ^{13}C-containing, was desorbed.* A control experiment, in which the system was initially purged with He and then with H_2 prior to the onset of ^{13}CO pulsing, demonstrated identical behaviour to that shown in Fig. 2B, i.e., the desorption of ^{12}C-methanol. This clearly shows that following the helium purge a significant quantity of methanol precursor was still present on the catalyst. Thus suppression of the CO-induced displacement of methanol when the CO is pulsed into He strongly implies that the precursor species is hydrogen-deficient. CO destabilises the methanol precursor species and, when a plentiful supply of surface hydrogen is available, the unsaturated precursor undergoes hydrogenation and desorbs. The source of adsorbed hydrogen is

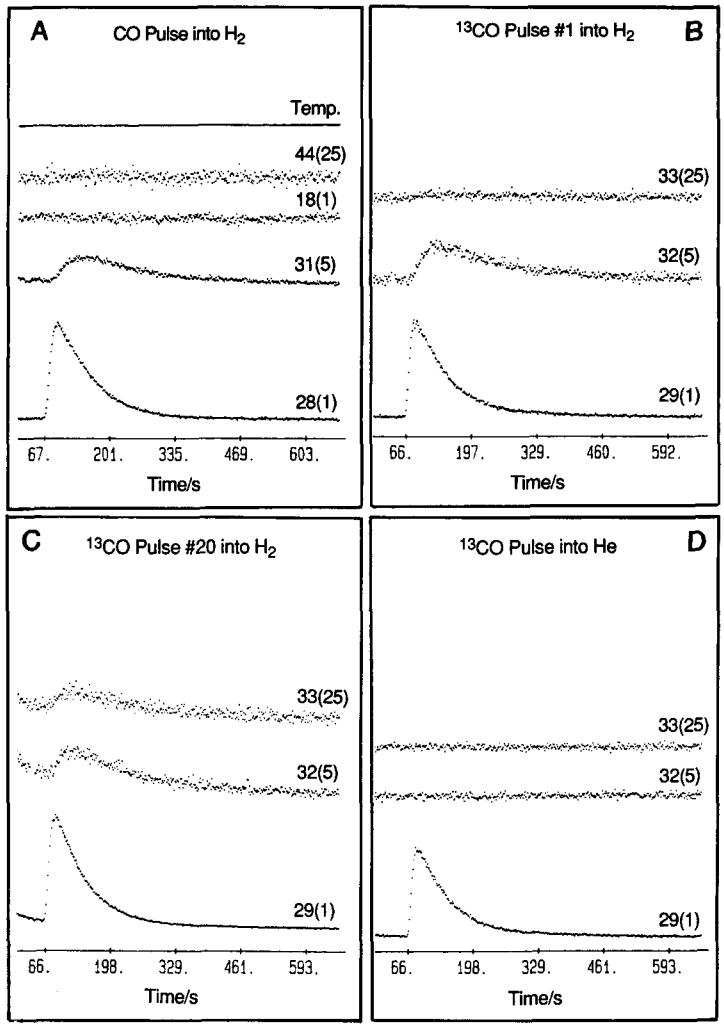

FIG. 2. Response to carbon monoxide pulsing at 180°C (A) Single ^{12}CO pulse into 14 bar H_2. (B) First ^{13}CO pulse into 14 bar H_2. (C) Twentieth ^{13}CO pulse in 14 bar H_2. (D) Single ^{13}CO pulse into 14 bar He. (Note: ^{13}CO pulses into a reduced flow rate of H_2 had been performed preceding the pulse shown in (C) to hasten the build-up of ^{13}CO-containing species).

absent when He is used as the carrier gas so displacement cannot occur.

The characteristics of the He-purge used in the control experiment (40 min/180°C) strongly implied that the precursor is *not* a formate species associated with copper sites alone, as proposed for $Cu/ZnO/Al_2O_3$ catalysts: the desorption half-life of formate on Cu is only ~5 s at 197°C (*15*). This is not to say that formate associated with interfacial CeO_x–Cu sites, or indeed with CeO_x sites alone, is not the precursor; it seems probable, however, that the precursor may be a species other than formate. In fact, a large amount of evidence ((*16*) and references therein) indicates that the mechanism of methanol synthesis over the industrial $Cu/ZnO/Al_2O_3$ catalyst is different in CO/H_2 and $CO/CO_2/H_2$ feeds. While the reaction proceeds via the formate intermediate in CO_2-containing feeds, sequential H addition to CO appears to occur in CO/H_2 alone.

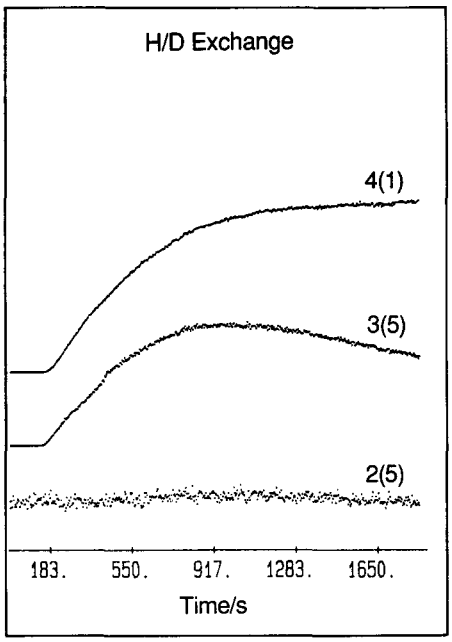

FIG. 3. H/D exchange in a 14-bar D_2 feed over a nitrogen-flushed catalyst activated in CO/H_2, all at 180°C.

The possible occurrence of $C^{18}O$–$C^{16}O$ exchange involving ^{16}O from the CeO_x lattice was also investigated. After activation and helium purging, the pulsing of $C^{18}O$ over the catalyst generated both $C^{16}O$ and (unreacted) $C^{18}O$ in the exit gas. Helium was used as carrier gas to exclude complications arising from the displacement of methanol which occurs in the presence of H_2; the methanol fragment at $m/e = 30$ would have complicated analysis of the $C^{18}O$ trace. The corresponding control experiment, pulsing ^{13}CO into He, also gave $^{12}C^{16}O$ in the exit stream, in approximately the same quantity as observed from the $C^{18}O$ pulse. This demonstrates that the unlabelled CO generated by the $C^{18}O$ pulse arises from the displacement of adsorbed, unlabelled CO from the catalyst surface. Thus there is no evidence for oxygen exchange with the oxide lattice.

Pulsing $C^{18}O$ into a hydrogen stream gave results completely consistent with those described earlier for pulsing ^{13}CO. That is, $CH_3{}^{16}OH$ was observed exclusively in the initial stages, but as more pulses were sent over the catalyst the level of $CH_3{}^{18}OH$ generated by a given pulse gradually rose. Once again, the results indicated the absence of direct oxygen exchange with the catalyst surface.

The lability of hydrogen on the catalyst and within the methanol precursor(s) was investigated in a series of experiments using deuterium. An alloy sample was activated in the usual way until steady state methanol synthesis activity was observed. The reactor (still at 180°C) was then flushed using 14 bar nitrogen before switching to a pure D_2 feed at 14 bar and Fig. 3 illustrates the response of the system to this. The $m/e = 3$ (HD) trace clearly demonstrates that H/D exchange is facile over the catalyst, and that the amount of exchange reaches a maximum, subsequently decreasing with time, the HD peak eventually returning to its baseline value. Once this had occurred, a pulse of unlabelled CO was injected into the D_2 stream. The resulting product distribu-

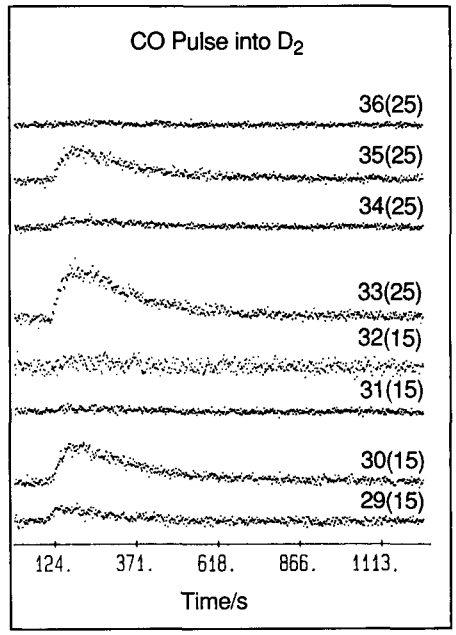

FIG. 4. Distribution of isotopically labelled methanol fragments resulting from pulsing CO into D_2 at 180°C.

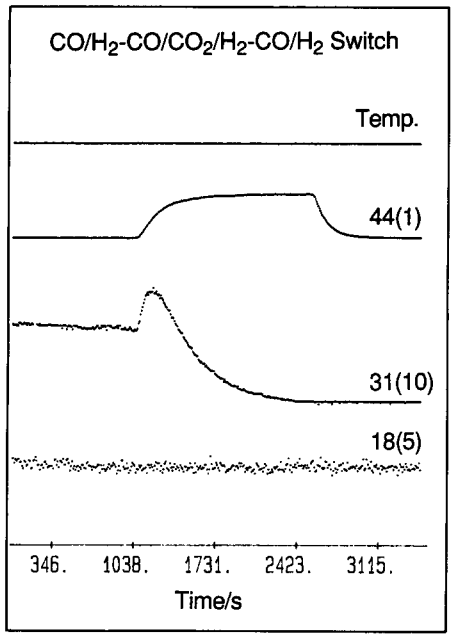

FIG. 5. Effect of temporarily switching from a (1 : 2) CO/H_2 feed to $CO/CO_2(2\%)/H_2$, all at 20 bar, 180°C.

tion is shown in Fig. 4. The data appear to be completely consistent with displacement of CD_3OH (m/e = 35); the mass spectral cracking pattern observed is identical to that expected for CD_3OH (*17*). However, the presence of CD_3OH on the catalyst surface in the presence of a large excess of D_2 would be rather surprising. Control experiments involving the pulsing of CD_3OD into a D_2 stream, revealed that the hydroxyl D undergoes complete exchange with residual H_2O in the sampling and analysis system. Such mass-spectrometer-related hydroxyl exchange of CD_3OD has been observed by other authors (*17*). We may therefore conclude that the precursor species covering the catalyst surface under methanol synthesis conditions probably undergoes complete H exchange with gas-phase D_2. In addition, it is noted that the CO-induced displacement of deuterated methanol into a D_2 feed is as facile as that of ^1H methanol into H_2.

CO_2 Pulsing

Low levels (<2%) of CO_2 in the CO/H_2 feed gas to methanol synthesis catalysts derived from rare earth–copper alloys are known to induce severe poisoning (*7, 9, 18*). For some systems (including the present $CeCu_2$-derived catalyst) this deactivation is both complete and irreversible.

Figure 5 shows the results obtained when the gas feed over a catalyst at steady-state activity was switched from 20 bar CO/H_2 to 20 bar $CO/CO_2/H_2$ (32 : 2 : 64) at 180°C. Immediately after the switch there is a large transient increase in the methanol yield, but this is followed by a rapid drop to a very low level of activity. No increase in activity was seen when the gas feed was switched back to the CO/H_2 mixture. No exotherm was associated with the introduction of CO_2; nor was there an increase in the level of water leaving the reactor, which shows that the reverse water–gas shift reaction,

$$CO_2 + H_2 = CO + H_2O, \qquad (1)$$

did not occur to any significant extent.

Figure 6 illustrates the effects of pulsing $^{13}CO_2$ into a CO/H_2 gas stream at 180°C over

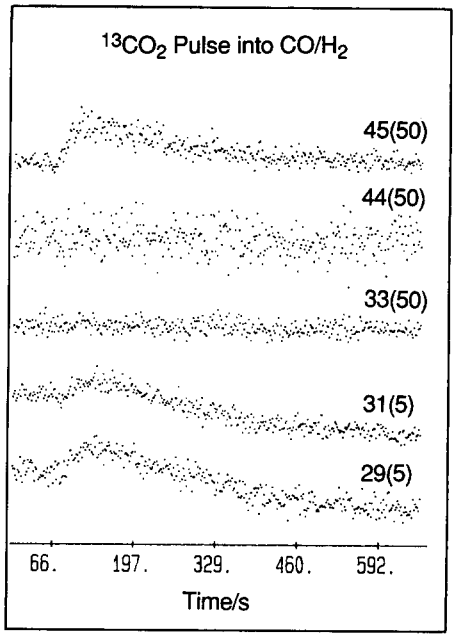

FIG. 6. Response of a catalyst operating under steady-state conditions (20 bar (1 : 2) CO/H_2, 180°C) to a pulse of $^{13}CO_2$.

a fresh catalyst operating at steady state activity. The $^{12}CH_3OH$ trace (m/e = 31) shows that there is a marked increase in the level of methanol in the exit gas before it returns to a new steady-state level which is only slightly lower than its original one. Most important is the fact that no $^{13}CH_3OH$ is observed (m/e = 33), which conclusively proves that *the transient increase in methanol yield is exclusively due to the displacement of preformed surface species from the catalyst*. That is, the $^{13}CO_2$ is merely a displacing agent—it is not directly incorporated into methanol product. In addition, it is clear that the catalyst is partially poisoned by the $^{13}CO_2$ in the pulse, since the steady-state level of methanol activity is reduced by the exposure. The $^{13}CO_2$ does not displace any $^{12}CO_2$, nor was there evidence for generation of water—in agreement with the $CO/CO_2/H_2$ data presented above. A comparison of the mass-31 and mass-29 traces reveals that the intensity of the pulse-induced transient in the 29 trace is too large to be due to methanol alone. This point is considered below.

As further $^{13}CO_2$ pulses were sent over the catalyst the amount of unreacted $^{13}CO_2$ passing through the system increased. At the same time the quantity of methanol desorbed per pulse exhibited a gradual decrease, as did the steady-state level of methanol activity in between pulses. After 25 pulses a low level of pulse-induced $^{13}CH_3OH$ (in addition to ^{12}C-methanol) was detectable: as explained below, this methanol is not thought to result from direct hydrogenation of $^{13}CO_2$, rather it appears to be due to the gradual build-up of ^{13}C-containing methanol precursor species on the catalyst surface.

TPD spectra from an active catalyst, from one poisoned using the $CO/CO_2/H_2$ gas mixture and from one partially poisoned by 20 pulses of $^{13}CO_2$ into CO/H_2, are shown in Fig. 7. In each case the catalyst was cooled from reaction temperature (180°C) to ambient temperature under CO/H_2. All three systems evolved large quantities of H_2, CH_4, and CO at high temperature and in no case was water desorbed. The principal differences between the three systems are manifest in the methanol and carbon dioxide traces. The active catalyst (Fig. 7A) exhibits a large, broad methanol desorption feature at low temperatures; very little CO_2 desorbed and no features were evident in the 33-amu and 45-amu traces. The catalyst poisoned in the $CO/CO_2/H_2$ gas feed gave the TPD profiles shown in Fig. 7B. The amount of methanol desorbed is greatly reduced relative to that observed from the active catalyst, and in addition, a significant quantity of CO_2 is desorbed at around 275°C. This temperature is too high for the CO_2 to be associated with either clean or partially oxidised Cu (*16*): it must therefore be associated with the CeO_x support in some way. The TPD data from the $^{13}CO_2$-poisoned catalyst (Fig. 7C) are broadly consistent with those obtained after exposure to the $CO/CO_2/H_2$ mixture. The feature at 29 amu is due to the desorption of ^{13}CO, since the 31-amu trace reveals that it cannot be methanol-related. Significant quantities of $^{13}CH_3OH$ were not desorbed. The $^{12}CO_2$ (44-amu) traces in Figs. 7A and 7C are very similar, which clearly shows that the $^{13}CO_2$ pulsing has no effect on the (very low) level of CO_2 that is invariably present on the active catalyst. This CO_2 associated with the active catalyst appears to be bound more strongly than is the subsequently pulsed CO_2.

Pulsing $^{13}CO_2$ into an H_2 stream gave very similar results to those obtained by pulsing $^{13}CO_2$ into CO/H_2. However, the CO/H_2 experiments did not allow an investigation of the response of adsorbed CO to a $^{13}CO_2$ pulse due to the very high level of gaseous CO present; this problem does not arise with a pure hydrogen feed. It has already been established that pulsing ^{13}CO into H_2 (or He) leads to the displacement of ^{12}CO. Figure 8A shows the results obtained when $^{13}CO_2$ was pulsed into an H_2 stream. As expected, a large quantity of ^{12}C-methanol was observed, but no $^{13}CH_3OH$ was desorbed. (The

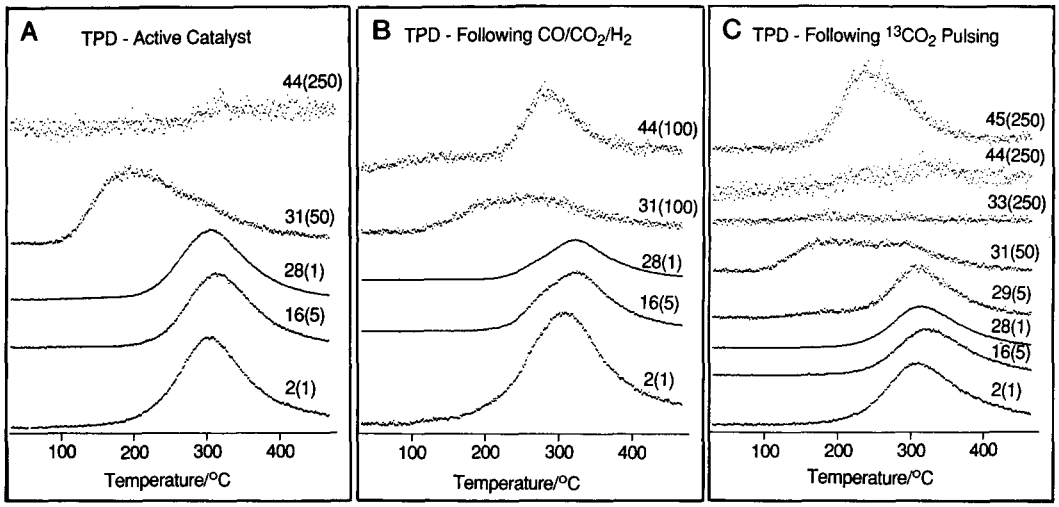

FIG. 7. Temperature-programmed desorption spectra: (A) active catalyst (B) catalyst poisoned by $CO/CO_2/H_2$ feed (see Fig. 5); (C) catalyst poisoned by a series of $^{13}CO_2$ pulses into a CO/H_2 feed.

small feature present in the 33-amu trace is consistent with the natural abundance of ^{13}C. A peak of the same intensity was also observed at 33 amu when $^{12}CO_2$ was pulsed into H_2.) It is clear that some CO is desorbed, although whether this CO is due to displacement or reaction is not immediately apparent. Once again the ratio of the intensities of the 29 and 31 peaks exceeds that expected if the 29 peak is due entirely to the CHO fragment of methanol. In addition, the methanol yield per pulse of CO_2 (Fig. 8A)

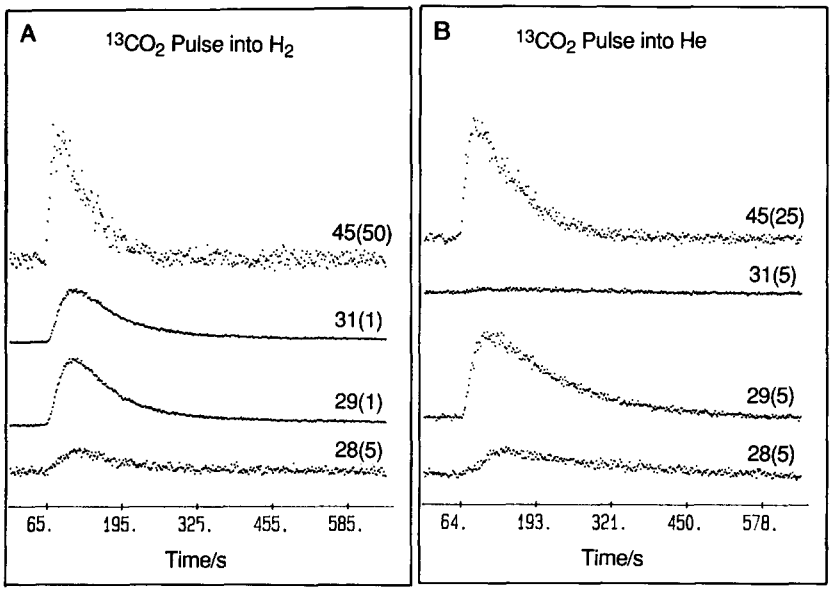

FIG. 8. Response of active catalyst to $^{13}CO_2$ pulses at 180°C: (A) H_2 feed; (B) He feed.

exceeds that per pulse of CO (Figs. 2A and 2B) by a factor of ~5, indicating that the interaction of CO_2 with the catalyst is significantly stronger than that of CO.

The processes leading to the desorption of CO are best explored by pulsing $^{13}CO_2$ into He, since no methanol is displaced under such conditions; the 29-amu trace will not then be complicated by the presence of the intense methanol-related 29-amu $(CHO)^+$ signal. Figure 8B shows the effect of pulsing $^{13}CO_2$ into a He stream: signals are observed at both 29 and 28 amu. The 29-amu feature cannot be methanol-derived (see 31-amu trace), and must therefore arise in one of two ways. Either it is due to the cracking of $^{13}CO_2$ to $^{13}CO^+$ in the mass spectrometer or it is caused by the generation of ^{13}CO as the $^{13}CO_2$ pulse passes over the catalyst. The first explanation may be ruled out, since the 45 and 29 traces do not have the same shape. In addition, calibration experiments gave a value of ~4 : 1 for the 45/29 ratio from pure $^{13}CO_2$. Thus ^{13}CO is generated during the passage of $^{13}CO_2$ over the catalyst. Three different mechanisms may be invoked to account for this. Firstly, the reverse water–gas shift reaction (Eq. (1)) could be responsible. Metallic Cu has high activity for the shift reaction and the formation of CO from CO_2 under methanol synthesis conditions is frequently ascribed to the reverse shift reaction. We do not believe that this is the case for the present system since (i) there is no detectable evolution of water, which would be stoichiometric on the amount of CO produced, and (ii) the only hydrogen present during these experiments was that which was held on the catalyst. The second possibility is the reverse Boudouard reaction,

$$^{13}CO_2 + {}^{12}C = {}^{13}CO + {}^{12}CO, \qquad (2)$$

i.e., the CO_2 burns off predeposited carbon from the catalyst surface. However, if this were the only reaction leading to generation of ^{12}CO then the $^{13}CO/^{12}CO$ ratio from the first $^{13}CO_2$ pulse sent over the catalyst would

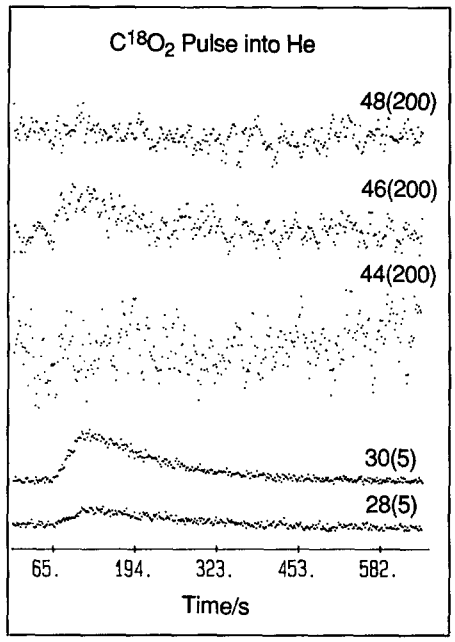

FIG. 9. Effect of pulsing $C^{18}O_2$ into an He feed at 180°C.

be unity. Figure 9 shows that this is clearly not the case. The most likely remaining possibility is the simple dissociative process

$$^{13}CO_2(g) \rightarrow O(a) + {}^{13}CO(g). \qquad (3)$$

Reaction (3) is believed to be important in determining the extent of oxidation of the Cu surface in the industrial $Cu/ZnO/Al_2O_3$ catalysts operating under $CO/CO_2/H_2$ (*16*). However, the present results indicate that CO_2 does not dissociate solely on Cu sites, since the resulting O(a) would be rapidly removed in CO/H_2 (*16*), leaving the Cu surface free to dissociate the next pulse of CO_2 with the same efficiency. The fact that the extent of the dissociation reaction was observed to *decrease rapidly with each successive pulse* argues strongly against such Cu-induced CO_2 dissociation. Note that CO_2 dissociation has also been reported over a Pt/CeO_2 catalyst (*19, 20*) for which it was established that the Pt–CeO_2 interface was the active site for reaction. It was found that no CO was formed when pure CeO_2 was

exposed to CO_2, and that the CO generated by CO_2 dissociation on the Pt/CeO_2 sample was bonded to Pt in the same manner as that found when the catalyst was exposed directly to CO. The evidence suggests that participation of CeO_2 oxygen vacancies adjacent to the Pt site is crucial—the oxygen atom from CO_2 fills the vacancy and the resulting CO spills over to the Pt. In the present case, any CO generated by such a mechanism which spills over to Cu will desorb immediately under synthesis conditions (*16*), unless it is incorporated into a methanol precursor species. The detection of some $^{13}CH_3OH$ after ~25 pulses of $^{13}CO_2$ into CO/H_2 would then be explicable in terms of $^{13}CO_2 \rightarrow {}^{13}CO$ conversion: a fraction of this ^{13}CO undergoes hydrogenation to ^{13}C-methanol. The intensity decrease of the 29-amu signal and the opposite behaviour of the 45-amu signal are also consistent with this explanation—as the number of oxygen vacancies decreases the probability of $^{13}CO_2$ dissociation also decreases. The build-up of ^{13}C-containing species on the catalyst can also be clearly seen in the TPD data of Fig. 7C, which shows significant desorption of ^{13}CO from the catalyst surface following extensive $^{13}CO_2$ pulsing.

The intensity variation of the 28-amu signal in the $^{13}CO_2$ pulsing experiments mirrored that of the 29-amu signal, decreasing as the number of pulses increased. However, none of the observations described thus far allows an unambiguous determination of the mode of generation of this unlabelled CO. If some of the $^{13}CO_2$ pulsed is indeed involved in carbon removal (Eq. (2)) then pulsing $C^{18}O_2$ should lead to the following reaction:

$$C^{18}O_2 + C = 2C^{18}O; \qquad (4)$$

that is, *no $C^{16}O$ should be seen.* Figure 9 shows the effect of pulsing $C^{18}O_2$ into He over an activated catalyst—note that $C^{16}O$ is observed. The presence of this unlabelled CO can only be accounted for in terms of displacement (since $C^{18}O$ has been shown not to undergo oxygen exchange), whilst the $C^{18}O$ is principally generated by the dissociation of $C^{18}O_2$ on the catalyst.

During the first $C^{18}O_2$ pulse significant oxygen exchange occurred to give $C^{18}O^{16}O$; Fig. 9 shows that the quantity of $C^{18}O^{16}O$ detected exceeds that of $C^{18}O_2$. (The $C^{18}O_2$ was only available in small quantities so that the pulsing pressure was significantly reduced: the 44-, 46-, and 48-amu traces have therefore been amplified and digitally smoothed). In subsequent pulses the $C^{18}O^{16}O/C^{18}O_2$ ratio gradually decreased until it reached the impurity level of $C^{18}O^{16}O$ in the original sample of gas. At the same time, the amount of $C^{18}O_2$ passing unreacted through the catalyst bed increased—by the fifth pulse the intensity of the 48 trace had risen by a factor of 20. Low levels of $C^{16}O_2$ were detected in subsequent pulses, showing that double oxygen substitution is also possible. The intensity of the $C^{16}O_2$ feature was, however, always significantly lower than that of the $C^{18}O^{16}O$, consistent with a low probability of readsorption and further exchange, although the gradual ^{18}O enrichment of the surface which occurs must also be a factor contributing to the low $C^{16}O_2/C^{18}O^{16}O$ ratio. Quantitatively similar oxygen-exchange phenomena were also seen when $C^{18}O_2$ was pulsed into a CO/H_2 stream.

In summary, the $C^{18}O_2$ can react with the catalyst in one of two ways; a given molecule can either break up on the surface to yield $C^{18}O$ or it can exchange an oxygen. This exchange presumably takes place on the CeO_x support since, in the absence of CO_2 in the gas feed, the exposed surface of copper crystallites will be fully reduced under reaction conditions (*16, 21–23*). The intermediacy of $C^{18}O$ in the exchange process can be ruled out since pulsing pure $C^{18}O$ over the catalyst did not generate any CO_2 species. It is most likely that exchange proceeds via a CO_3 intermediate; the probability of formation of this species may in turn be determined by the extent of oxide reduction and oxygen-vacancy concentration.

The increase in amount of $C^{18}O_2$ passing unreacted through the system in successive

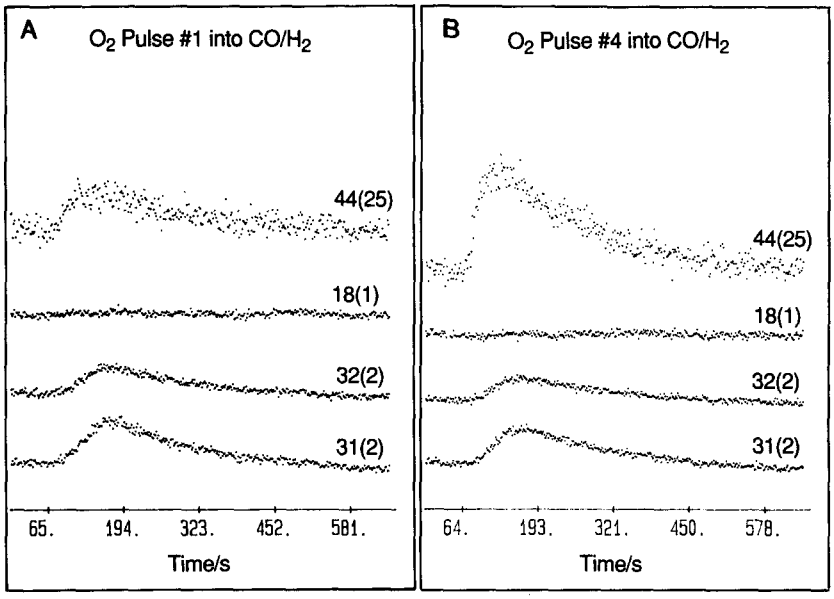

FIG. 10. Response of active catalyst to O_2 pulsing into a 20-bar CO/H_2 feed at 180°C: (A) first pulse; (B) fourth pulse.

pulses probably reflects a decrease in the sticking probability of the $C^{18}O_2$. This decrease (which is also evident in the $^{13}CO_2$ data) appears to be driven by the reaction of CO_2 with the catalyst surface—possible reasons are discussed later. There is a strong correlation between the probabilities of CO_2 adsorption, oxygen exchange, and CO_2 dissociation which suggests the influence of a common determining factor.

O_2 Pulsing

Figure 10A illustrates the effect of pulsing O_2 into a CO/H_2 feed to a catalyst exhibiting steady state methanol synthesis activity. No oxygen passes through the catalyst bed unreacted; the 32/31 amu intensity ratio is fully consistent with the observed 32-amu peak being entirely attributable to the molecular ion of methanol—indeed, methanol is the main "product" of the first pulse. The oxygen does not react to generate water, but a small amount of CO_2 is produced. The activation energy of the Langmuir–Hinshelwood reaction between CO and O_2 on Cu is 6 kcal/mol (*23*) so any oxygen which dissociates on Cu will be removed very rapidly by gas-phase CO: this could be the origin of the observed CO_2. The CO_2 level gradually increased with pulse number. Figure 10B shows the transient effects arising from the fourth O_2 pulse into CO/H_2 over the catalyst. The methanol yield is slightly lower than that obtained from the first pulse, but the CO_2 level is significantly higher. It is possible that a similar amount of CO_2 was produced by the first pulse and that most of it reacted further with the catalyst. The alternative explanation for the gradual increase in the level of detected CO_2 is that a larger proportion of the O_2 in the early pulses is used in direct oxidation of CeO_x vacancies rather than being converted into CO_2 over the catalyst. During subsequent pulses more of the oxide surface is in an oxidised state, with a reduced sticking probability for oxygen, so more O_2 is available to react on the Cu with CO to give CO_2. Clearly, the catalyst is poisoned by the O_2 pulses, since steady-state methanol production is consistently lower once the pulse has passed.

Figure 11A shows the TPD spectra ob-

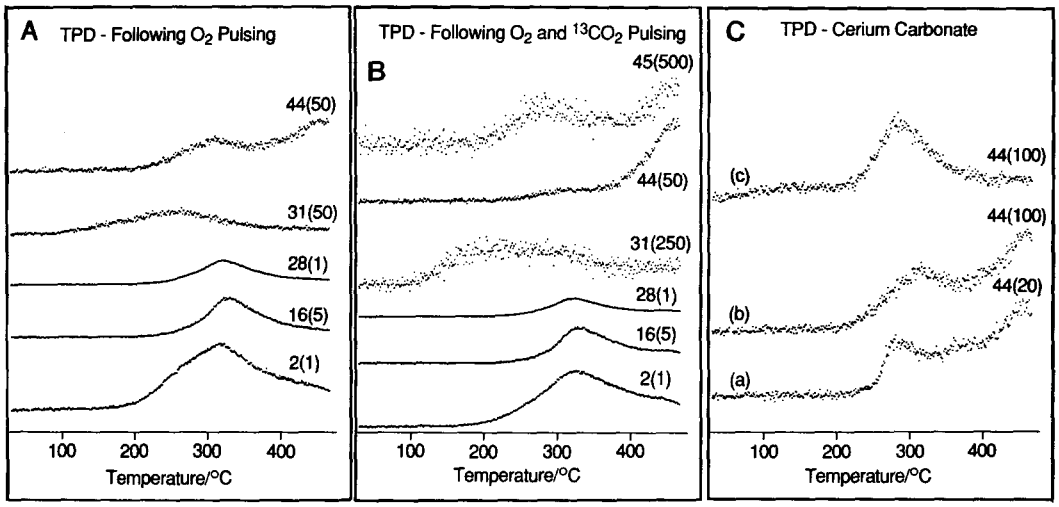

FIG. 11. Temperature-programmed desorption spectra: (A) catalyst poisoned by multiple O_2 pulses into a CO/H_2 feed; (B) catalyst poisoned by exposure to four pulses of O_2 followed by a sequence of $^{13}CO_2$ pulses (all into CO/H_2); (C) CO_2 (44 amu) TPD traces from (a) bulk cerium carbonate, (b) catalyst poisoned by O_2 pulsing, and (c) catalyst poisoned by steady-state $CO/CO_2/H_2$ treatment.

tained from a catalyst following exposure to a series of O_2 pulses in a CO/H_2 gas stream. A comparison with the corresponding traces from CO_2-poisoned catalysts (Figs. 7B and 7C) shows that the hydrogen, methane, CO and methanol signals from O_2- and CO_2-poisoned systems are very similar. The most significant difference between the two sets of data is seen in the CO_2 traces. The characteristic "fingerprint" of CO_2-poisoned catalysts is the intense CO_2 desorption peak at ~275°C. When oxygen is used to induce the poisoning, this peak is still present, but an additional, higher temperature CO_2 desorption feature of greater intensity is also apparent.

Further information on the effects of oxygen exposure was obtained by partially poisoning a catalyst using O_2 (4 pulses into CO/H_2) and then pulsing $^{13}CO_2$ (again into CO/H_2) over this modified system. The response of the system to the first $^{13}CO_2$ pulse in this sequence may be compared with that of an active catalyst to the fifth pulse of $^{13}CO_2$; in both cases, some ^{13}CO was generated, some $^{12}CH_3OH$ was displaced, and some $^{13}CO_2$ passed unreacted through the system. The differences are in the magnitude of these effects—a smaller amount of methanol was displaced from the partially O_2-poisoned system, and a larger amount of $^{13}CO_2$ passed through unreacted. These observations are consistent with the greater displacing and oxidising power of O_2. Consequently, the response of the partially O_2-poisoned (4 pulses) catalyst to the $^{13}CO_2$ pulse is equivalent to that of an activated catalyst exposed to 15–20 $^{13}CO_2$ pulses. The TPD spectra obtained following ten $^{13}CO_2$ pulses over the partially O_2-poisoned catalyst are shown in Fig. 11B. Virtually all of the $^{12}CO_2$ originates from the high binding energy state: this unlabelled desorption product can only be associated with the adsorption of carbon dioxide generated during catalyst activation and by the reaction of CO with pulsed O_2. The subsequently pulsed $^{13}CO_2$ which adsorbs on the catalyst populates both the high and low binding energy states.

These two sets of data (Figs. 11A and 11B), in conjunction with that presented in Fig. 7, reveal that oxygen induces significant changes in the CO_2-related behaviour of the catalyst. The role of the oxygen is *not* simply

to undergo conversion to CO_2, thereby indirectly deactivating the catalyst. The more marked effects of oxygen exposure may in part be associated with the strongly exothermic interaction of the gas with the catalyst. Such an exotherm would not have been detected in this work since the thermocouple was only in contact with the external surface of the reactor tube for all the O_2 pulsing experiments. Previous work (*14*), however, has shown that switching from pure He to pure O_2 at atmospheric pressure and 200°C over an active $CeCu_2$-derived catalyst can induce an increase in catalyst bed temperatures of 200°C. In the present case, dilution of the O_2 (1 : 20) and the transient nature of the dose ensure that any exotherm will be much smaller. However, the occurrence of an exotherm could in part explain why six times more methanol is displaced by pulsing oxygen into a CO/H_2 stream than by pulsing the same pressure of CO_2.

To facilitate interpretation of the CO_2 data described above, experiments were carried out on a sample of cerium carbonate that had been pretreated in 20 bar CO/H_2 at 180°C for 2 h. Figure 11C(a) shows the resulting TPD trace, along with the spectra obtained from extensive O_2 poisoning and $CO/CO_2/H_2$ treatment of the alloy-derived catalyst, traces (b) and (c), respectively. The two peaks in trace (a) appear to be due to the initial liberation of CO_2 from the surface of the carbonate, followed, at higher temperature, by bulk decomposition of the sample. Whether the low temperature feature is related to strongly adsorbed CO_2 or to a surface carbonate phase is not clear. The overall similarity of traces (a) and (b) implies that the O_2 pulsing leads to the formation of a bulk-like cerium carbonate phase in the alloy-derived catalyst, while trace (c) indicates that treatment in CO_2-containing feeds merely results in the generation of a surface carbonate phase (or simply an adsorbed layer of CO_2). There are a number of possible reasons why oxygen exposure (and not CO_2 exposure alone) is necessary for the formation of a bulk carbonate. One possibility is that complete oxidation to near-stoichiometric CeO_2 is a prerequisite to nucleation of bulk carbonate, and this is only achieved at the high oxygen activities present during a pulse of O_2 gas. Alternatively, the differences may be associated with the markedly greater exothermicity of the interaction of oxygen with the catalyst surface. It is possible, for example, that an O_2-induced exotherm facilitates the break up of the CeO_x surface, so the CO_2 can more easily enter to generate several layers of carbonate.

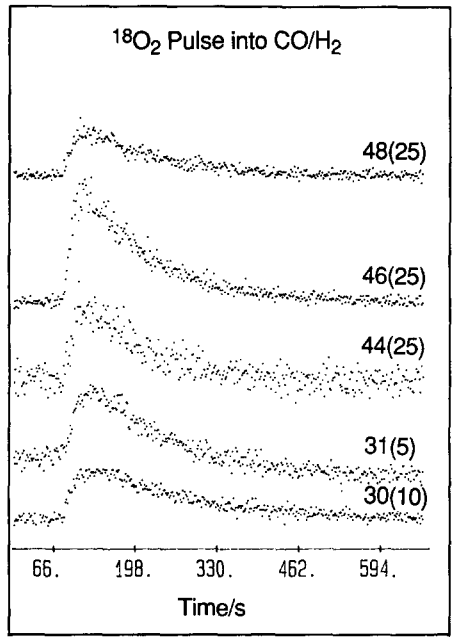

FIG. 12. Effect of pulsing $^{18}O_2$ onto a catalyst exhibiting steady-state methanol production from CO/H_2 at 180°C.

Additional information was obtained from an experiment in which $^{18}O_2$ was pulsed into CO/H_2 over a catalyst operating at steady state activity. Figure 12 shows the results. No $^{18}O_2$, $^{18}O^{16}O$, or $^{16}O_2$ were detected but, as expected, $CH_3{}^{16}OH$ displacement was observed. The most intense CO_2-related signal is due to $C^{16}O^{18}O$, which may then undergo oxygen exchange, either with oxygen already present on the catalyst (to give $C^{16}O_2$) or with further ^{18}O, yielding $C^{18}O_2$.

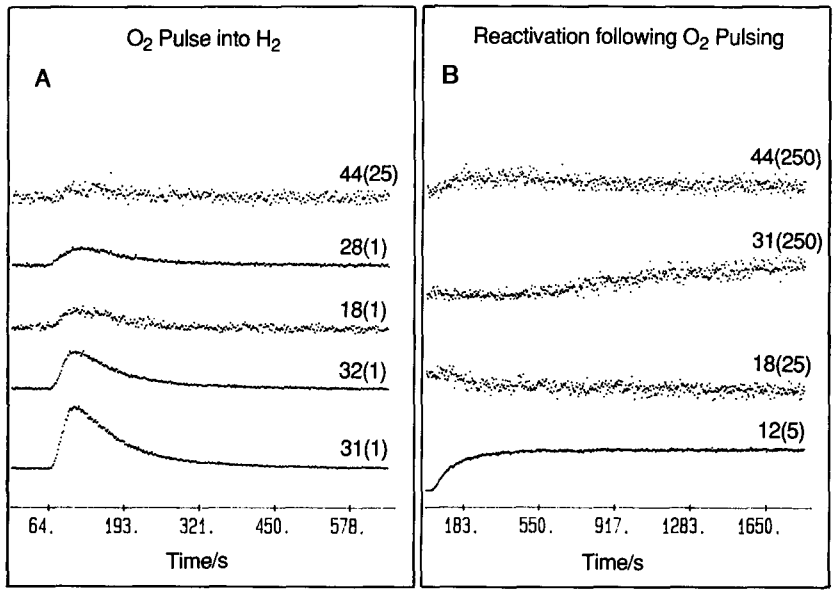

FIG. 13. (A) Response of active system to pulsing O_2 into a pure H_2 feed at 180°C. (B) Slow, partial reactivation of the catalyst (poisoned by O_2 pulsing into hydrogen) after switching back to a 20-bar CO/H_2 feed.

From the intensity ratio of the three CO_2-related features, it appears that the probability of such further exchange is not as high as that of direct passage through the catalyst. In addition, exchange with ^{16}O seems to be more likely than exchange with ^{18}O. The exchange of oxygen in $C^{18}O_2$ has already been described (Fig. 9), and we may again conclude that the ^{16}O involved in the further exchange to yield $C^{16}O_2$ is CeO_x-derived, since any ^{16}O on Cu would be rapidly removed by reaction with CO. By the third pulse the level of $C^{18}O_2$ exceeded that of $C^{16}O_2$, as expected from the gradual build-up of ^{18}O on the oxide surface. CO_2 dissociation is also clearly occurring, since the 30-amu trace contains a significant contribution from the $C^{18}O$.

The results obtained when O_2 was pulsed into an H_2 stream over the activated catalyst at 180°C are shown in Fig. 13A. This time only a very small amount of CO_2 is desorbed—either via O_2-induced displacement or from further reaction of displaced CO. Once again a large quantity of methanol is displaced, and no oxygen survives passage through the catalyst bed. In the absence of CO in the gas feed, the oxygen also reacts with hydrogen producing water. After ten O_2 pulses the gas feed was switched from H_2 to CO/H_2: Fig. 13B shows that almost complete deactivation had occurred. The steady-state activity ultimately obtained was approximately 100 times lower than that of the freshly generated system.

DISCUSSION

One of the main findings of this study is that under synthesis conditions the catalyst surface is extensively covered by methanol precursor species. These species desorb as methanol when CO, CO_2, and O_2 are pulsed into H_2 streams, and when CO_2 and O_2 are pulsed into CO/H_2 feeds. The hydrogen-deficient nature of the precursor species is shown by the experiments in which CO and CO_2 were pulsed into He—under such conditions no methanol was displaced.

If the transient increase in methanol yield observed when CO_2 is introduced into the

CO/H_2 feed (Fig. 5) is due entirely to the displacement of preformed methanol and methanol precursor species, as the $^{13}CO_2$ pulsing data clearly imply, then the number of molecules of methanol contained within this transient provides information about the surface concentration of these species under operating conditions. The transient is equivalent to ca. $2–3 \times 10^{20}$ molecules/g · cat, corresponding to saturation coverage of ~20–30 m^2/g of catalyst surface. It is extremely unlikely that this amount of methanol could be associated purely with the exposed copper surface of the catalyst (*24*), which means that the CeO_x surface must also be covered with methanol and methanol precursor species under steady-state conditions. The presence of a methanol precursor pool extending onto the surface of the oxide component has also been proposed for the industrial $Cu/ZnO/Al_2O_3$ methanol synthesis catalyst (*25*). In the present case it is not clear whether this methanol pool is actually formed on the oxide surface, or whether the initial stages of the synthesis reaction occur on the Cu, before spillover to the support occurs. Frost's junction effect theory (*26*) would predict that it is the former which occurs, whilst the more traditional view of methanol synthesis would favour the latter postulate.

Relatively little detailed information is available regarding the detailed nature of the CeO_x which is generated by intermetallic decomposition. Our recent *in situ* XAS study (*8*) of this material showed that Ce does not fully attain the +4 oxidation state characteristic of bulk CeO_2, although the fluorite structure of the oxide is evident in X-ray and electron diffraction patterns (*7, 18*). Quantitative analysis of the H_2 TPD data shows that a large amount of hydrogen is present within the bulk of the support phase. It is therefore likely that the properties of this CeO_x material are significantly different from those of pure CeO_2, which is inactive for methanol synthesis at 180°C (*27*). The possibility that highly defective CeO_x generates methanol without the involvement of the Cu species is precluded by observations made on catalysts derived from CeAg, $CeAg_2$, $CeCu_{1.3}Ag_{0.66}$ (*28*), and from $CeAu_2$ (*27*), where a similar CeO_x support phase is generated, but without low-temperature methanol synthesis activity.

The exact role of the copper species remains unclear. Chinchen *et al.* (*16, 21, 22*) reported a linear correlation between methanol synthesis activity and N_2O-titrated copper surface area not only for Cu/Al_2O_3, Cu/ZnO, and $Cu/ZnO/Al_2O_3$ catalysts, but also for other supports including SiO_2 and MgO. These results were taken as proof that the active centres are located exclusively on copper particles and that the main role of the oxide is that of structural promoter. However, the possible role of oxide-induced N_2O decomposition was not fully considered. The observations of Chinchen *et al.* contradict earlier work of Klier and co-workers (*29*) which indicated that a synergistic effect operated, the zinc oxide having a unique role in determining methanol synthesis activity. More recently, Burch and co-workers (*30, 31*) have clearly demonstrated a support-dependent effect for Cu/ZnO, Cu/SiO_2, and Cu/ZrO_2 catalysts. On the other hand, Frost's junction effect theory (*26*) proposes that the crucial chemistry occurs entirely on the oxide phase and that the role of the metal component is simply to promote electronically the productivity of the oxide. In support of this hypothesis, Frost showed that it was possible to generate active catalysts based on thoria-supported Ag and Au—metals which are normally considered to be inactive for methanol synthesis. He proposed that ionised vacancy sites on the oxide support are responsible for methanol synthesis activity and that the concentration of such sites is increased by the formation of a Schottky junction between the transition metal and the oxide.

One apparent strength of the junction effect theory is its ability to predict the changes in reactivity induced by switching the gas feed from CO/H_2 to $CO/CO_2/H_2$. For

a given transition metal (in this case Cu) Frost showed that the ratio of activity in CO/H_2 to that in $CO/CO_2/H_2$ was strongly dependent on the enthalpy of formation of the oxide making up the support. A high enthalpy of formation implies that the stoichiometric oxide is difficult to reduce and is therefore readily oxidized if initially present in its reduced state; a feed gas containing CO_2 will therefore greatly decrease the oxygen vacancy concentration and hence the methanol synthesis activity. The preceding argument is, of course, based on thermodynamic quantities, which can only provide a guide to likely kinetic behaviour. Productivity ratios (defined as the ratio of activities in CO/H_2 prior to, and immediately after, exposure to a CO_2-containing feed) for Cu/ZnO, Cu/ZrO_2, and Cu/ThO_2 were 0.8, 4, and 10, respectively, while the normalised enthalpies of formation (i.e., per mole of O atoms) of the oxides are -350, -553, and -616 kJ/mol, respectively. However, data obtained by Jennings *et al.* (*9*) show that this relationship is not strictly adhered to for catalysts generated from rare earth–Cu alloys. Of the catalysts investigated, two were totally and irreversibly poisoned by CO_2-containing feed. Clearly this corresponds to a very high productivity ratio, while the enthalpies of formation of the relevant oxides (La_2O_3 and CeO_2) are -601 and -544 kJ/mol. The two catalysts which generated significant levels of methanol from the $CO/CO_2/H_2$ feed (and therefore had low productivity ratios) had *greater* enthalpies of formation, namely, -610 (Gd_2O_3) and -624 kJ/mol (Dy_2O_3). These relatively small differences in enthalpies of formation between the systems irreversibly poisoned by CO_2 and those which generate methanol under such conditions become even smaller when one takes account of the XAS observation that the $CeCu_2$-derived catalyst appears to contain predominantly Ce^{3+} (*8*); the normalised enthalpy of formation of Ce_2O_3 is -602 kJ/mol. Nevertheless, the trend is that the catalyst with the *lowest* productivity ratio (Dy_2O_3/Cu) has the *highest* normalised enthalpy of formation of the oxide, i.e., the exact opposite of what would be expected according to the junction effect theory. Nevertheless it remains true that the principal effects associated with the switch from CO/H_2 to $CO/CO_2/H_2$ observed by Frost with a conventionally prepared ThO_2/Cu catalyst—a large initial transient of methanol followed by a rapid fall in activity to a level below that in CO/H_2—closely resembles that observed in this work and in other work on $RECu_2$-derived catalysts (*7, 9, 14*). Hitherto no explanation for the initial rise in methanol yield has been proposed; this study has clearly shown that it is due to the CO_2-induced displacement of preformed methanol and methanol precursor species from the surface.

Besides the anion vacancy model, other hypotheses have been put forward to explain the effect of CO_2. These include carbonate formation and irreversible (or partially irreversible) CO_2 adsorption on the basic rare earth oxides (*9, 14*). The evidence presented both in this paper and in earlier papers strongly suggests that Cu particles do not constitute the only active site in these alloy-derived catalysts. If they did, one might expect an *increase* in activity when the gas feed was changed from CO/H_2 to $CO/CO_2/H_2$ (as opposed to the drastic decrease observed). The presence of gas-phase CO_2 does reduce the oxygen vacancy concentration (as predicted by Frost (*26*)), but this is not its sole function. The principal effect of the CO_2 appears to be associated with its tendency to bind strongly to the CeO_x surface, thereby blocking adsorption sites. This leads to a drastic reduction in catalytic activity, indicating that the oxide surface is involved in the reaction. Quantification of the TPD data reveals that the amount of CO_2 desorbing following the $CO/CO_2/H_2$ treatment ($2–5 \times 10^{19}$ molecules) is of the order of a monolayer. This observation, along with the TPD data from the cerium carbonate and O_2-poisoned catalyst, clearly demonstrates that bulk carbonate formation does *not* occur in CO/

CO_2/H_2 gas feeds under the conditions of this study.

The $^{13}CO_2$ pulsing data reveal that a significant proportion of the initial CO_2 which reacts with the catalyst does so dissociatively with the liberation of CO. We have shown that this process must involve the CeO_x phase and conclude that the oxygen atoms generated by CO_2 dissociation become associated with the CeO_x phase. The surface stoichiometry of the CeO_x will therefore approach the CeO_2 stoichiometry characteristic of the highest oxidation state of Ce. During the initial stages of CO_2 poisoning a large volume of methanol is also desorbed; this is consistent with the presence of a substantial quantity of methanol and its precursors on the CeO_x surface. A significant proportion of this methanol would thus appear to be associated with the oxygen vacancies—vacancy filling by CO_2 dissociation leading to methanol displacement. As the methanol concentration decreases and the oxide surface stoichiometry approaches CeO_2, CO_2 dissociation declines and irreversible CO_2 adsorption commences, possibly forming a surface carbonate phase. This leads to irreversible poisoning. The very low residual level of methanol generated over the CO_2-poisoned catalyst is probably due to the Cu particles alone.

The results of Jennings *et al.* (*9*) for other alloy-derived catalysts can be interpreted in a similar way. They found that at 50 bar and 240°C both Gd_2O_3/Cu and Dy_2O_3/Cu generated methanol when 1–2% CO_2 was present in the gas feed, while La_2O_3/Cu, CeO_x/Cu, and Nd_2O_3/Cu catalysts did not. Earlier work (*32*) on crystalline rare earth oxides showed that the rate of CO_2 desorption at a given temperature was higher for Gd_2O_3 and Dy_2O_3 than for Nd_2O_3 and La_2O_3; the rate for CeO_2 was much higher than for any of the other oxides. However, XAS results (*8*) show that the $CeCu_2$-derived catalyst has an oxide stoichiometry closer to Ce_2O_3. Clearly, these observations made over crystalline rare earth oxides are not necessarily directly transferable to the alloy-derived catalysts, where the oxides exhibit a high degree of disorder. Nevertheless, the trend predicted from the CO_2 adsorption data is followed by the catalysts' response to CO_2. It seems, therefore, that CO_2 poisons the reaction by strong adsorption on the rare earth oxide phase. If this CO_2 desorbs at an appreciable rate under $CO/CO_2/H_2$ synthesis conditions (as appears to be the case with Gd_2O_3/Cu and Dy_2O_3/Cu catalysts) then some methanol activity will persist in such feeds. If, however, the CO_2 adsorption is essentially irreversible under reaction conditions, then catalytic activity will be greatly reduced—since only bare Cu sites will remain available for methanol generation.

The strength of CO_2 adsorption and operating temperature of the catalyst are also the principal parameters determining the extent of recovery of activity after switching back to a CO_2-free gas feed. In the specific case of the CeO_x/Cu catalysts, it has been previously noted (*14*) that the poisoning is irreversible, since significant desorption of the carbon dioxide cannot be achieved at temperatures below those at which thermal deactivation occurs. The present results corroborate those obtained from a $^{14}CO_2$ radiotracer experiment performed over a catalyst derived from a Ce/Cu/Al alloy (*9*), which demonstrated that methanol was formed from CO and not CO_2 in a $CO/CO_2/H_2$ feed. We have shown that some of the labelled $^{13}CO_2$ is eventually converted into product methanol, but only because a fraction of this CO_2 dissociates over the CeO_x support, yielding ^{13}CO which subsequently generates ^{13}C-containing methanol. The radiotracer experiments cited above demonstrated that the proportion of methanol containing ^{14}C was identical to the proportion of ^{14}C-containing CO.

RE alloy-derived catalysts therefore behave quite differently from the industrial catalytic system, where the methanol is generated almost exclusively from CO_2 in CO_2-containing feeds (*12*). Denise and Sneeden (*33*) have proposed that with supported copper catalysts there are two routes to metha-

nol—one from CO/H_2 and one from CO_2/H_2. They showed that the support plays a crucial role in determining which of the two paths is followed. Their Cu/MgO, Cu/La_2O_3, and Cu/Sm_2O_3 catalysts were far more active in CO/H_2 than in CO_2/H_2. Cu supported on potassium-promoted ThO_2 was shown to be active in both feeds, but exhibited significantly higher activity in the CO/H_2 mixture. Cu/ZnO and Cu/Al_2O_3 both possessed high activities in CO_2/H_2, but were inactive towards CO/H_2. In the light of our results it appears likely that strong CO_2 adsorption on the basic rare earth oxide- and MgO-supported catalysts is at least partially responsible for the observed low activity of these catalysts in CO_2/H_2. This conclusion would appear to be confirmed by the observation that the activity of the Cu/MgO catalyst dropped by a factor exceeding 10 when 3.6% CO_2 was introduced into the CO/H_2 feed (*34*). Adsorption of CO_2 is *reversible* over the Cu/MgO catalysts (*34*), and the replacement of a CO_2/H_2 feed by CO/H_2 led to a marked recovery in activity, to a level comparable to that obtained prior to the CO_2/H_2 treatment. The results of Denise and Sneeden (specifically the observation that rare earth oxide-supported catalysts were most active in CO/H_2 feeds) are therefore consistent with our findings that the alloy-derived rare earth oxide-supported Cu catalysts generate methanol from CO. Catalyst reponse to CO_2 may also be rationalised in these terms—catalysts incorporating basic supports are most active when CO_2 is excluded from the feed gas; even very low levels of CO_2 severely reduce catalytic activity. It appears therefore that the mechanism by which these catalysts generate methanol *from* CO/H_2 mixtures involves participation of the support; when support sites are blocked by CO_2 adsorption the activity drops significantly.

CONCLUSIONS

(1) The principal route to methanol over RE alloy-derived catalysts involves hydrogenation of CO and not CO_2.

(2) The catalyst surface is extensively covered with a methanol precursor (and possibly methanol itself) under conditions of steady-state synthesis—there is evidence that hydrogenation of this precursor or the desorption of methanol itself is rate limiting.

(3) Transient increases in the exit concentration of methanol may be achieved by *displacement* of methanol from the catalyst surface using pulses of CO, CO_2, and O_2 into H_2-containing feed gas streams. The efficiency with which these gases displace methanol decreases in the order

$$O_2 > CO_2 > CO.$$

(4) A large reservoir of *absorbed* hydrogen also exists within the catalyst—this readily exchanges with gas phase hydrogen but does not itself act as the source of hydrogen necessary for pulse-induced displacement of methanol.

(5) Carbon dioxide interacts with the CeO_x component of the catalyst in a number of ways:

(i) dissociative adsorption yielding gas-phase CO and resulting in oxidation of the surface of the CeO_x phase;

(ii) oxygen exchange, probably through a "CO_3" surface intermediate;

(iii) strong adsorption on the CeO_x surface when $x \rightarrow 2$.

In the presence of gas phase O_2, nucleation of a bulk-like cerium carbonate can also occur.

More generally, it is proposed that the surface of the CeO_x phase or the interface of this phase with copper crystallites is intimately involved in the synthesis mechanism. Whilst the small Cu crystallites are an essential part of the catalytic system, they alone are not able to propagate rapid synthesis from CO/H_2.

The strength of adsorption of carbon dioxide on the oxide surface is crucial in determining the response of the catalysts to CO_2 in the feed gas; specifically, it controls the synthesis activity under such conditions and also the rate of recovery upon returning

to a pure CO/H_2 feed. There is evidence that this behaviour is common to a wide range of different methanol synthesis catalysts.

ACKNOWLEDGMENT

APW acknowledges financial support under an SERC Postdoctoral Research Fellowship.

REFERENCES

1. Takeshita, T., Wallace, W. E., and Craig, R. S., *J. Catal.* **44,** 236 (1976).
2. Imamura, H., and Wallace, W. E., *Proc. Symp. Cat. Reactions involving Syn Gas ACS* 82 (1980).
3. Barrault, J., Duprez, D., Percheron-Guegan, A., and Achard, J. C., *Appl. Catal.* **5,** 99 (1983).
4. Barrault, J., Guilleminot, A., Achard, J. C., Paul-Boncour, V., Percheron-Guegan, A., Hilaire, L., and Coulon, M., *Appl. Catal.* **22,** 273 (1986).
5. Wallace, W. E., France, J., and Shamsi, A., *in* "Rare Earths in Modern Science and Technology," Vol. 3. Plenum, New York, 1982.
6. Baglin, E. G., Atkinson, G. B., and Nicks, L. J., *Ind. Eng. Chem. Prod. Res. Dev.* **20,** 87 (1981).
7. Nix, R. M., Rayment, T., Lambert, R. M., Jennings, J. R., and Owen, G., *J. Catal.* **106,** 216 (1987).
8. Shaw, E. A., Rayment, T., Walker, A. P., Lambert, R. M., Gauntlett, T., Oldman, R. J., and Dent, A., *Catal. Today* **9,** 197 (1991).
9. Jennings, J. R., Lambert, R. M., Nix, R. M., Owen, G., and Parker, D. G., *Appl. Catal.* **50,** 157 (1989).
10. Bridger, G. W., and Spencer, M. S., *in* "Catalyst Handbook" (M. W. Twigg, Ed.), 2nd ed., Chap. 9. Wolfe, London, 1988.
11. Kagan, Y. B., Rozovskii, A. Y., Liberov, L. G., Slivinskii, E. V., Lin, G. I., Loktev, S. M., and Bashkirov, A. N., *Dokl. Akad. Nauk SSSR* **224,** 1081 (1975).
12. Chinchen, G. C., Denny, P. J., Parker, D. G., Spencer, M. S., and Whan, D. A., *Appl. Catal.* **30,** 333 (1987).
13. Jennings, J. R., Owen, G., Nix, R. M., and Lambert, R. M., *Appl. Catal. A* **82,** 65 (1992).
14. Nix, R. M., Judd, R. W., Lambert, R. M., Jennings, J. R., and Owen G., *J. Catal.* **118,** 175 (1989).
15. Bowker, M., Hadden, R. A., Houghton, H., Hyland, J. N. K., and Waugh, K. C., *J. Catal.* **109,** 263 (1988).
16. Chinchen, G. C., Spencer, M. S., Waugh, K. C., and Whan, D. A. *J. Chem. Soc. Faraday Trans 1* **83,** 2193 (1987).
17. Akhter, S., Cheng, W. H., Lui, K., and Kung, H. H., *J. Catal.* **85,** 437 (1984).
18. Owen, G., Hawkes, C. M., Lloyd, D., Jennings, J. R., Lambert, R. M., and Nix, R. M., *Appl. Catal.* **33,** 405 (1987).
19. Jin, T., Okuhara, T., Mains, G. J., and White, J. M., *J. Phys. Chem.* **91,** 3310 (1987).
20. Jin, T., Zhou, Y., Mains, G. J., and White, J. M., *J. Phys. Chem.* **91,** 5931 (1987).
21. Chinchen, G. C., and Waugh, K. C., *J. Catal.* **97,** 280 (1986).
22. Chinchen, G. C., Waugh, K. C., and Whan, D. A., *Appl. Catal.* **25,** 101 (1986).
23. Habraken, F. H. P. M., and Bootsma, G. A., *Surf. Sci.* **87,** 333 (1979).
24. Whilst the small copper particle size derived from XRD (*7*) and EXAFS (*8*) implies a high Cu area, gas adsorption studies show that the *available* area is low. The *in situ* N_2O-titratable Cu surface area of the active catalyst is $\lesssim 1$ m^2/g (*14*). Reducing the sample at 240–300°C leads to a significant increase in N_2O decomposition; however, we believe this may be associated with H_2-induced removal of species from the surface of the CeO_x at high temperature. The "additional" N_2O then breaks up over the nonstoichiometric oxide surface exposed by this hydrogen treatment. BET measurements of the total surface area are also consistent with a relatively small area of exposed Cu (*18*).
25. Jackson, S. D., and Brandreth, B. J., *J. Chem. Soc. Faraday Trans. 1* **85,** 3579 (1989).
26. Frost, J. C., *Nature* **334,** 577 (1988).
27. Shaw, E. A., Walker, A. P., Rayment, T., and Lambert, R. M., *J. Catal.*, in press.
28. Shaw, E. A., Rayment, T., Walker, A. P., Jennings, J. R., and Lambert, R. M., *J. Catal.* **126,** 219 (1990).
29. Herman, R. G., Klier, K., Simmons, G. W., Finn, B. P., Bulko, J. B., and Kobylinski, T. P., *J. Catal.* **56,** 407 (1979).
30. Bartley, G. J. J., and Burch, R., *Appl. Catal.* **43,** 141 (1988).
31. Burch, R., and Chappell, R. J., *Appl. Catal.* **45,** 131 (1988).
32. Artamonov, E. V., and Sazonov, L. A., *Kinet. Katal.* **12,** 961 (1971).
33. Denise, B., and Sneeden, R. P. A., *Appl. Catal.* **28,** 235 (1986).
34. Denise, B., Cherifi, O., Bettahar, M. M., and Sneeden, R. P. A., *Appl. Catal.* **48,** 365 (1989).